Molecular dynamics studies of entangled polymer chains

Bulacu, Monica Iulia

Chapter 2

Basic concepts of polymer physics

It doesn't matter how beautiful your theory is, it doesn't matter how smart you are. If it doesn't agree with experiment, it's wrong.

Richard Feynman

This chapter contains a short introduction into the polymer physics that is indispensable in understanding many polymer applications. It starts with the description of the microscopic static and dynamic properties of polymer chains. To describe the polymer conformations that are specific for polymer chains in dense polymeric systems, isolated chain models are introduced. Then, the basic principles of polymer dynamics are presented as they emerge from two fundamental theories: Rouse and reptation. Since the microscopic properties and behavior strongly influence the macroscopic properties of polymeric materials, some general details of the glass transition of amorphous polymers are illustrated. The chapter ends with a brief description of an application where both microscopic and macroscopic properties are evidently revealed: polymer adhesion.

2.1 Polymer chain topology and characterization

Polymers are large molecules formed by extremely many atoms linked together by covalent bonds. They are synthesized by joining together, in a systematic way, groups of relatively light and simple molecules generically named *monomers*. After such a linkage process, called polymerization, the obtained polymers can have very different topologies: linear chains, rings, combs, or networks. It is due to the large diversity of constitutive parts (mostly carbon, hydrogen, nitrogen grouped together in various monomers) and to the countless topologies that very different polymers exist and exhibit a wide range of properties.

This thesis is restricted to synthetic polymers such as poly(methyl methacrylate)–PMMA (acrylic glass or Plexiglas) or polystyrene–PS which are linear polymers (without branches) (Fig. 2.1).

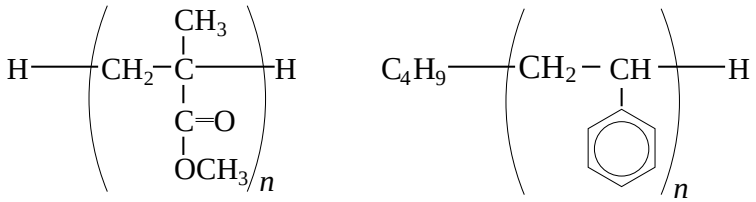

Poly(methyl mehtacrylate) Polystyrene

Figure 2.1: *Poly(methyl methacrylate) (PMMA) and polystyrene (PS). n corresponds to the number of repeat units.*

At first glance a linear polymer with N monomers connected by $N-1$ bonds (in Fig. 2.2) is a random coil with N steps.

To describe the configuration of a polymer we have to know the location in space of each monomer: $3N$ Cartesian coordinates XYZ with respect to the laboratory fixed frame. This description has the advantage of simple calculation of the inter-atomic distances and chain specific measures. Various simplified measures of a chain's configuration are in use. The simplest is the end-to-end vector $\mathbf{R}(N)$ connecting the first and the last beads from the chain:

$$\mathbf{R}(N) = \mathbf{r}_1 - \mathbf{r}_N \tag{2.1}$$

A more precise characteristic that uses more than just the end beads, is the radius of gyration defined as

$$\mathbf{R}_{\mathrm{g}}^2(N) = \left\langle (\mathbf{r}_i - \mathbf{r}_{\mathrm{CM}})^2 \right\rangle \tag{2.2}$$

where $\mathbf{r}_i$ is the position vector of bead number i in the chain and $\mathbf{r}_{\mathrm{CM}}$ is the position vector of the center of mass of the polymer chain; the symbol $\langle\rangle$ represents the mean over all N beads from the chain.

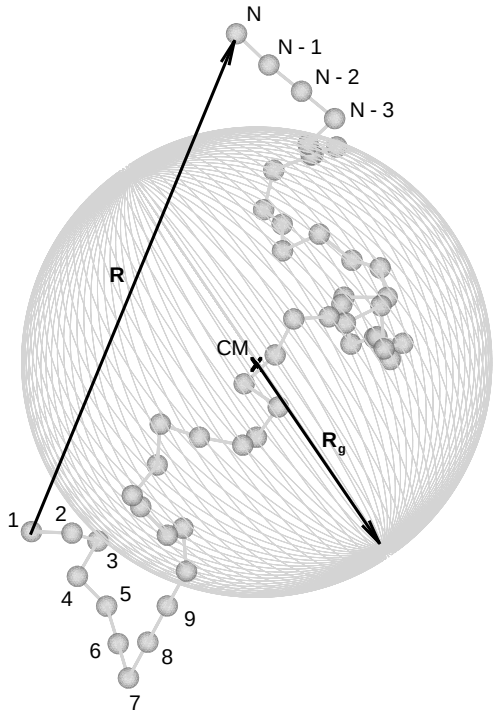

Figure 2.2: *The representation of a linear polymer chain with N monomer units, characterized by its end-to-end distance $\mathbf{R}$ and its radius of gyration $\mathbf{R}_{\mathrm{g}}$. CM denotes the center of mass of the chain.*

The Cartesian description of the chain conformation is a very good tool for polymer characterization and molecular dynamics. But the nature of the polymer itself offers a more intuitive representation. The location of a monomer $(i+1)$ along the chain is completely defined by three internal measures relative to the previous monomers i and $i-1$: the bond length b_i between monomer i an $i+1$, the bending angle θ_i made by b_i with b_{i+1} and the dihedral angle ϕ_i made by the plane $(b_i b_{i+1})$ with $(b_{i-1} b_i)$, as illustrated in Fig. 2.3. Depending on the specific polymer, these three internal measures are restricted to some values from a limited set. By knowing all of them we have the entire information about the chain conformation. The complete understanding of the shape of isolated polymer chain is valuable in developing analytical theories that describe physical properties of polymers.

2.2 Isolated polymer chain models

Polymers with very different chemical configurations may have similar properties or may undergo similar phenomena. The reason is that only some specific characteristics

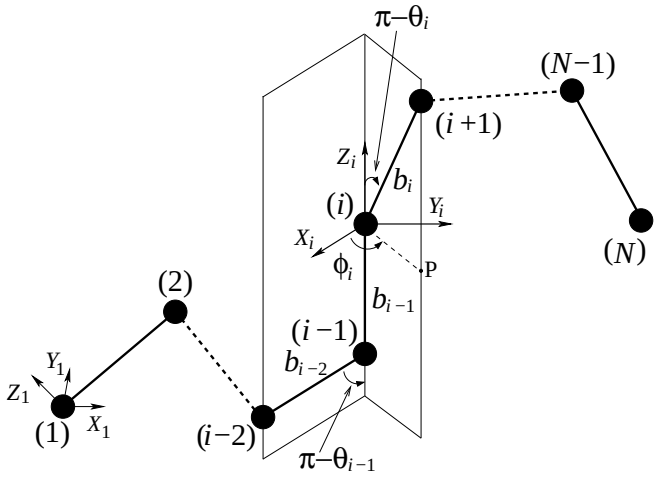

Figure 2.3: *Schematic representation of a polymer chain. Monomer indices are indicated in parentheses.* b_i *is the bond length,* θ_i *is the bending angle and* ϕ_i *is the dihedral angle. The local* $(X_iY_iZ_i)$ *coordinate system is such that* Z_i *is aligned with bond* b_{i-1}*;* X_i *lies in the plane defined by bonds* b_{i-1} *and* b_{i-2} *and makes an acute angle with* X_{i-1}*;* Y_i *completes a right-handed coordinate system. P is the projection of bead* $i+1$ *on the* (X_iY_i) *plane and allows for visualization of the dihedral angle* ϕ_i*.*

such as chain length, chain topology, etc., are responsible for the polymer behavior. This suggests the use of very simple general models for polymer chains in which the very fine chemical details are neglected.

The most popular simplified models of a polymer chain (Flory 1969) will be recapitulated in the subsequent sections.

2.2.1 Freely jointed chain (FJC)

In this simple model a polymer chain is represented as a succession of monomer units that interact only by covalent binding forces. As a result the bond length is fixed and the internal rotations are completely free. Evidently, this characterization obeys random flight model (Barber and Ninham 1970) and, implicitly, a long freely jointed chain will obey Gaussian statistics: the probability to observe a certain end-to-end vector $\mathbf{R}$ is given by the Gaussian distribution function with zero average (centered in the origin) and mean squared value:

$$\left\langle \mathbf{R}^2(N) \right\rangle \equiv \left\langle R^2(N) \right\rangle = Nb^2 \tag{2.3}$$

where b is the bond length and N is the number of bonds (since the number of beads N is usually a big number, no distinction is made between it and the real number of bonds $N-1$). Flory (1969) used this relation to define the characteristic ratio C_∞ of a polymer

as

$$C_\infty = \lim_{N\to\infty} \frac{\langle R^2(N)\rangle}{Nb^2}. \tag{2.4}$$

By definition, $C_\infty^{\mathrm{FJC}} = 1$. Values of C_∞ larger than 1 occur when some of the degrees of freedom are constrained. Then C_∞ can be used as a measure of stiffness along the polymer backbone.

2.2.2 Freely rotating chain (FRC)

This model is used when short-range interactions are considered between beads separated by a small number of valence bonds. The bond angles are fixed or narrowly fixed to constant values and the dihedral angles (rotational angles) are completely free. The characteristic ratio in this case is:

$$C_\infty^{\mathrm{FRC}} = \frac{1-\cos\theta}{1+\cos\theta}. \tag{2.5}$$

When all bending angles θ are restricted to $\theta_0 = 109.5°$, $C_\infty^{\mathrm{FRC}} = 2.0$ instead of 1 for unrestricted bending angles.

2.2.3 Rotational isomeric state (RIS)

Short-range interactions between the beads also influence the distribution of the dihedral angles along the chain. In reality, all dihedral angles are perhaps possible, but they prefer the low energy states. As a consequence, in addition to the constraints on bonds and bending angles, the dihedral angles have to be constrained as well. In a simplified rotational isomeric state model, they can take one of the three values: $\phi_0 = 60°$ (gauche$^+$), $\phi_0 = 180°$ (trans) and $\phi_0 = 300°$ (gauche$^-$). Thermal energy will allow the angles to overcome the energetic barriers and to make transitions from one state to the other. The population of all rotational angles, however, will not be equal: usually probabilities of 0.2, 0.6 and 0.2 are specific for gauche$^+$, trans and gauche$^-$, respectively. The characteristic ratio in this case is computed from:

$$C_\infty^{\mathrm{RIS}} = \frac{1-\cos\theta}{1+\cos\theta}\frac{1-\langle\cos\phi\rangle}{1+\langle\cos\phi\rangle} \tag{2.6}$$

and its value is 4.7

Polymer chains with constraints on bending angles (FRC) or on both bending and torsion angles (RIS) can be treated as completely unrestricted chains (FJC) by considering an effective bond length $b_{\mathrm{eff}}^2 = C_\infty b^2$. As a consequence, for each chain there is a length scale on which it appears like an FJC chain. This is possible since by increasing

the chain stiffness, only C_∞ changes but not the scaling of $\langle R^2(N)\rangle$ with N (Eq. (2.3)). For ideal chains, the radius of gyration can also be calculated:

$$\left\langle \mathbf{R}_{\mathrm{g}}^2(N)\right\rangle = \frac{1}{6}\left\langle \mathbf{R}^2(N)\right\rangle . \tag{2.7}$$

Despite their simplicity, Eqs. (2.3) and (2.7) are the most fundamental results of polymer science.

All the isolated chain models presented above address unperturbed chains i.e. chains whose conformation is unaffected by non-local interactions between groups of atoms that are distance apart along the chain. These "ideal chain" conformations are realized experimentally only in bulk amorphous polymers (the main subject of this thesis) and in dilute solutions under extremely special conditions (specific solvent, temperature).

When non-local interactions are also considered, the most suitable model is the self-avoiding random walk in which the chain bonds are not allowed to cross each other and the end-to-end distance scales as

$$\sqrt{\langle R^2(N)\rangle} \propto N^{\upsilon} \tag{2.8}$$

with $\upsilon = \frac{3}{2+d}$, in terms of the dimensionality d of the system ($\upsilon = 0.6$ in three dimensions instead of $\upsilon = 0.5$ according to Eq. (2.3)). Self-avoiding random walk is the best model when describing dilute polymer coils in solution, except for the exceptional case mentioned above where the chain is ideal and one of the three models (FJC, FRC or RIS) are more appropriate.

2.3 Chain dynamics in polymer melts

The dynamics of a separate polymer chain is by itself a very complex problem: the random motion of each bead is restricted by the chain connectivity and the interactions with other monomers, while the overall motion is the result of successive individual adjustments. Chain dynamics is even more complicated if the chain is part of a dense ensemble of other chains (in melts, glasses or networks): supplementary restrictions arise due to the chain entanglement. Different sub-parts of the chain have more or less freedom to rearrange depending on their length, to the extent that the overall conformations, characterized by end-to-end distance or radius of gyration, necessitate a very long time to forget their original values.

The motion of the chains inside a polymeric material is ultimately revealed in the macroscopic properties of the material, so that there is great interest in understanding chain dynamics.

Polymer dynamics can be suitably analyzed by monitoring the monomers and the chain centers of mass in time. More specifically, three mean-square displacements, of a system with M chains with N beads per chain, are often investigated:

- the absolute bead mean-square displacement, $g_1(t)$:

$$g_1(t) = \frac{1}{MN} \left\langle |\mathbf{r}_i(t) - \mathbf{r}_i(0)|^2 \right\rangle \; ; \tag{2.9}$$

- the bead mean-square displacement relative to the chain's center of mass, $g_2(t)$:

$$g_2(t) = \frac{1}{MN} \left\langle |\mathbf{r}_i(t) - \mathbf{r}_i(0) - \mathbf{r}_{\mathrm{CM}}(t) + \mathbf{r}_{\mathrm{CM}}(0)|^2 \right\rangle \; ; \tag{2.10}$$

- the mean-square displacement of the chain center of mass, $g_3(t)$:

$$g_3(t) = \frac{1}{M} \left\langle |\mathbf{r}_{\mathrm{CM}}(t) - \mathbf{r}_{\mathrm{CM}}(0)|^2 \right\rangle \; . \tag{2.11}$$

The self-diffusion coefficient D of the chains inside a polymer melt is computed from the slope of $g_3(t)$ using the Einstein relation

$$D = \lim_{t \to \infty} \frac{1}{6t} g_3(t) \, . \tag{2.12}$$

Two of the most widely used theories for polymer melt dynamics reduce the problem to a single chain motion in an effective medium: the *Rouse model* for the simple case of unentangled chains (Rouse 1953) and the *reptation model* for entangled chains (de Gennes 1979, Doi and Edwards 1989).

In the Rouse model, a Gaussian chain of beads connected by springs interacts with a stochastic medium that mimics the presence of the other chains. As a consequence, the chain center of mass is subjected to particle-like diffusion and the self-diffusion coefficient D is expected to reach the asymptotic value

$$D = \frac{k_{\mathrm{B}} T}{\zeta N}, \tag{2.13}$$

ζ being the effective bead friction coefficient, k_{B} the Boltzmann's constant and T the temperature.

In the reptation model, the polymer chain is confined inside a "tube" formed by the constraints imposed by the entanglements with other chains. One of the main predictions of this theory is the drastic slow down of the chain motion revealed by the self-diffusion coefficient:

$$D = \frac{1}{3} \frac{d_{\mathrm{T}}^2}{l^2} \frac{k_{\mathrm{B}} T}{\zeta N^2} \, , \tag{2.14}$$

where d_{T} is the tube diameter and l ($l^2 = C_\infty b^2$) is the effective bond length.

The change in the scaling of D from $D \propto N^{-1}$ according to the Rouse model to $D \propto N^{-2}$ predicted by the reptation model, at N_{e} is schematically represented in Fig. 2.4.

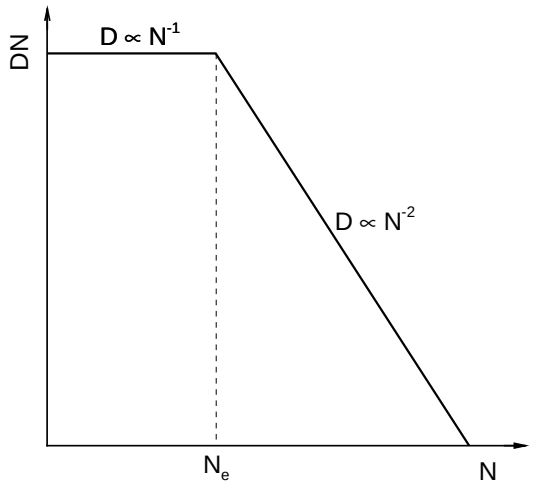

Figure 2.4: *Schematic representation of the chain length dependence of DN. This dependence is predicted theoretically to have a crossover from the Rouse regime to the reptation regime as the chains are long enough to entangle, $N \geq N_{\mathrm{e}}$.*

The theoretically expected behaviors for $g_1(t)$ and $g_3(t)$ in the Rouse and reptation models are also different. Within the Rouse model $g_3(t) \propto t$ for all times, while $g_1(t)$ has two visible regimes (de Gennes 1967):

$$g_1(t) \propto \begin{cases} t^{1/2} & \text{for} \quad \tau_0 < t < \tau_{\mathrm{R}} \\ t & \text{for} \quad t > \tau_{\mathrm{R}} \end{cases} \tag{2.15}$$

The crossover between these two regimes occurs at the Rouse time τ_{R} which is the time needed for a chain with N beads to diffuse over a distance equal to its mean radius of gyration, $g_1(\tau_{\mathrm{R}}) \approx \left\langle R_{\mathrm{g}}^2(N) \right\rangle$.

The reptation model predicts for the mean-square displacement of the chain center of mass $g_3(t)$ a similar sequence as the Rouse theory for $g_1(t)$:

$$g_3(t) \propto \begin{cases} t^{1/2} & \text{for} \quad \tau_{\mathrm{e}} < t < \tau_{\mathrm{R}} \\ t & \text{for} \quad t > \tau_{\mathrm{R}}, \end{cases} \tag{2.16}$$

and for $g_1(t)$ an extra, weaker time dependence $g_1(t) \propto t^{1/4}$ embedded inside the $t^{1/2}$ regime:

$$g_1(t) \propto \begin{cases} t^{1/2} & \text{for} \quad \tau_0 < t < \tau_{\mathrm{e}} \\ t^{1/4} & \text{for} \quad \tau_{\mathrm{e}} < t < \tau_{\mathrm{R}} \\ t^{1/2} & \text{for} \quad \tau_{\mathrm{R}} < t < \tau_{\mathrm{d}} \\ t & \text{for} \quad t > \tau_{\mathrm{d}} \end{cases} \tag{2.17}$$

The $t^{1/4}$ regime in Eq. (2.17) is usually considered as the reptation "fingerprint". Between the entanglement time $\tau_{\mathrm{e}} \approx \tau_{\mathrm{R}}(N_{\mathrm{e}})$ and the Rouse time τ_{R}, the chain moves like

a Rouse chain "trapped" inside a tube that materializes the constraints induced by the entanglements. The tube diameter is related to the radius of gyration of a chain with N_{e} beads through the relation $d_{\mathrm{T}}^2 \approx \langle R_{\mathrm{g}}^2(N_{\mathrm{e}})\rangle$. After τ_{R} the chain acts like a free Rouse chain with the usual $t^{1/2}$ and t^1 regimes and the crossover at the disentanglement time τ_{d}.

Figure 2.5 schematically represents the differences between the time dependences of $g_1(t)$ as predicted by these two theories.

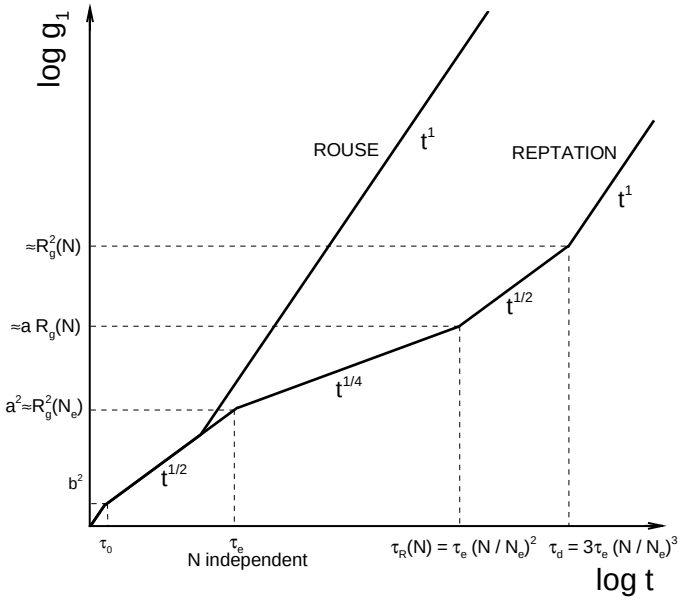

Figure 2.5: *Schematic representation of the time dependences of g_1 conform to the Rouse and reptation models.*

A mention has to be done here: only the inner parts of a polymer chains undergo a clear reptation motion (with g_1 dependence on time predicted by the Eq. (2.17)). The beads situated at the chain ends are more free to explore the space out of the tube. This behavior is investigated in more detail in (Chapter 4).

2.4 Glass transition

Polymeric materials are one of the most representative classes of materials that can exist in the glassy state. Such glasses are produced by cooling or compressing a highly viscous polymer liquid in such a way that crystallization is avoided and a microscopically disordered solid is obtained. It is noted that in reality a complete crystalline phase is an exception for polymers: they prefer to remain in the amorphous state or to have amorphous and crystalline sub-domains (semi-crystalline polymers).

The process of transition from a liquid to an amorphous solid (in the polymer as a whole or in its future non-crystalline domains) is called the glass transition. The temperature at which this transition occurs (actually a narrow temperature range specific for each material) is known as the glass transition temperature T_{g}. Since the polymer changes from a highly viscous liquid (or rubbery solid) to a rather brittle glassy material at all temperatures below T_{g}, this temperature is also referred to as the "brittle temperature".

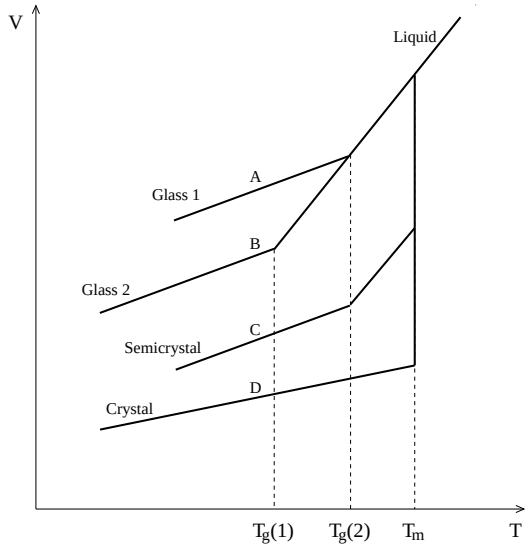

Figure 2.6: *Schematic representation of the specific volume V versus temperature T, upon cooling from the liquid melt in the case of fully amorphous polymers at high cooling rate (curve A) and low cooling rate (curve B), semi-crystalline polymer at high cooling rate (curve C) and crystalline polymer (curve D).*

Even though it is known for millennia how to vitrify liquids (beads of glass for jewelry were manufactured since 1500 BC, in Egypt), this phenomenon is still not completely understood theoretically. Besides cooling rate effects, what is more puzzling is that chemically very different liquids undergo the glass transition, no matter how various are their internal interactions (ionic, van der Waals, hydrogen bonds, covalent bonds or even metallic bonds).

One possible explanation of this process is that, as the liquid cools through its glass transition, the molecular motion is more and more retarded to the limit that the dynamical behavior of the liquid can no longer be distinguished from that of a solid on the time sale of the experiment. The molecules seem to be frozen-in, thus resulting in the amorphous structure of a glass. To measure the internal mobility inside the material, the macroscopic viscosity η is often used and traditionally the value of about 10^{13} poise (1 poise = 0.1 Nsm^{-2}) is considered a sign of the glass transition.

Another way to identify the glass transition is to monitor specific thermodynamic quantities that are known to have distinct "discontinuities" during the transition (e.g. specific volume, heat capacity). Fig. 2.6 gives such an example for how the specific volume can depend on temperature.

The knowledge of the glass transition temperature together with the melting temperature is very valuable information in the selection, improvement and design of polymer products in an industrial setting. This thesis is focused on polymers that are in the glassy state at room temperature (thermoplastic or glassy polymers): with examples like PMMA with $T_{\mathrm{g}} = 105°\mathrm{C}$ or PS with $T_{\mathrm{g}} = 95°\mathrm{C}$ (the given values are bulk glass transition temperatures). When one deals with surfaces or interfaces slightly different values of T_{g} are expected due to size-dependent surface/interface effects or to the ageing effects induced by the fact that the physical properties of the polymer change gradually with time, a glassy material not being in thermodynamic equilibrium.

2.5 Adhesion of polymers

Typically polymers are immiscible: when two polymers are bonded together very few chains diffuse from one polymer bulk to the other, as is represented in Fig. 2.7.

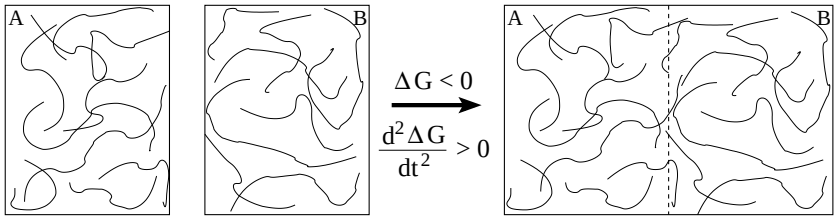

Figure 2.7: *A representation of the adhesion process of two polymer bulks A and B. When A and B are in contact at the joining temperature chains from bulk A diffuse into bulk B and chains from bulk B diffuse into bulk A providing that the two conditions indicated in the figure for the Gibbs free energy are fulfilled.*

As a result the interpenetration distance of the chains is very small and a reasonable adhesion cannot be achieved. The grade of immiscibility of two polymers is related to the chain length (polymers with longer chains are more immiscible), the specific volume fractions of the two polymers and, the interaction between two units belonging to the two species. Two polymers will bond if the Gibbs free energy of mixing (per segment) satisfies $\Delta G < 0$ and $\frac{d^2\Delta G}{dt^2} > 0$. For the calculation of the Gibbs free energy an approximative expression can be used– the Flory-Huggins formulation:

$$\frac{\Delta G(\varphi)}{k_B T} = \frac{\varphi}{N_A}\ln\varphi + \frac{(1-\varphi)}{N_B}\ln(1-\varphi) + \chi\varphi(1-\varphi). \tag{2.18}$$

with N_A and N_B the degrees of polymerization for polymers A and B, φ the volume fraction of polymer A segments and χ the Flory segment-segment interaction parameter. Since usually N_A and N_B are large numbers and χ between any two polymers chosen randomly is positive, Eq. (2.18) indicates a strong immiscibility for typical polymer pairs.

One strategy to increase the adhesion between such polymers is to improve the natural entanglement at the interface by adding supplementary connecting molecules usually block copolymers (Creton et al. 2001). Some parts of these connectors diffuse into one bulk, and the rest in the other bulk, effectively sewing the interface. When the adhesion is then broken, it is assumed that all the stress transfer is done by the connector chains.

During adhesion fracture the connectors can suffer different mechanisms: simple pull-out, scission or crazing (they can form fibrils that are pulled-out from the process zone until the connector chains from these may be pulled-out or broken). A very intuitive picture of the fracture mechanisms depending on the connector length and the areal density of the connectors is given in Fig. 2.8, as proposed by Creton et al. (2001).

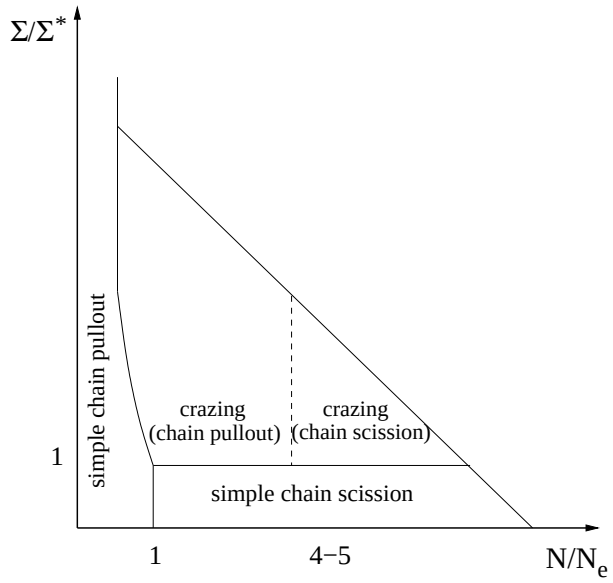

Figure 2.8: *Fracture mechanism map for the interface between glassy polymers reinforced with connector chains.* N_e *is the entanglement length of the connector chains and* Σ^* *is the areal density at which the crazing phenomenon appears in the systems (conform with Fig. 53 from Creton et al. (2001)).*